

Conformational and optical properties of macromolecules of some aliphatic-substituted cellulose esters

N. V. Tsvetkov · S. V. Bushin · M. A. Bezrukova ·
E. P. Astapenko · N. G. Mikusheva · E. V. Lebedeva ·
A. N. Podseval'nikova · A. K. Khripunov

Received: 29 October 2012 / Accepted: 13 March 2013 / Published online: 23 March 2013
© Springer Science+Business Media Dordrecht 2013

Abstract Synthesized cellulose pelargonates, tridecanoates, valerates, and acetovalerates of various molecular weights are studied in chloroform, dioxane, and tetrachloroethane solutions by the methods of isothermal translational diffusion, sedimentation velocity method, flow birefringence (dynamooptical Maxwell effect), viscometry, and equilibrium electric birefringence (Kerr effect). The equilibrium polymer rigidities are determined and the role of the solvent and temperature in the formation of the conformational characteristics of the macromolecules under study is analyzed. The values of the intrinsic optical anisotropy of the monomeric units of the studied cellulose esters are experimentally determined. The contribution of the side chains to the optical anisotropy of the macromolecules of cellulose esters with aliphatic substituents is analyzed. The results obtained in this study are compared with the data on the cellulose esters with the aliphatic side substituents studied earlier. For the studied samples, the values of

the longitudinal components of the monomeric unit dipoles in a nonpolar solvent are estimated.

Keywords Macromolecule conformation · Aliphatic groups · Cellulose · Maxwell effect · Kerr effect

Introduction

To a great extent, the interest in the cellulose esters (CE) is associated with their use as binding agents, additives, modifiers, film-forming materials in the processing of plastics, woodworking, and leather working (Edgar et al. 2001). Cellulose esters make up a broad class of thermoplastics with diverse properties (Steinmeier 2004). Among the conventional application areas of CE (acetates, butyrates) are the production of textile fibers, plastics, and films (Borgan and Brewer 1985; Klemm et al. 1998), as well as various coatings, because CEs reduce the drying time, improve smoothing, add lustre, are stable carriers for metal pigments, and enhance the UV stability (Edgar et al. 2001). The amphiphilic properties of the aliphatic-substituted cellulose combined with the high equilibrium rigidity of molecules make it an attractive object for producing single- and multilayer Langmuir–Blodgett nanofilms (Stepina et al. 2005; Tredgold 1987), which can be successfully used in micro- and nanoelectronics, analytical biotechnology, bioelectronics, and membrane technologies (Khripunov

N. V. Tsvetkov (✉) · N. G. Mikusheva ·
E. V. Lebedeva · A. N. Podseval'nikova
Department of Physics, St. Petersburg State University,
Ul'janovskaja street 1, 198504 St. Petersburg, Russia
e-mail: N.Tsvetkov@mail.ru

S. V. Bushin · M. A. Bezrukova · E. P. Astapenko ·
A. K. Khripunov
Institute of Macromolecular Compounds, Russian
Academy of Sciences, Bol'shoj prospect 31,
199004 St. Petersburg, Russia

et al. 2000; Stepina et al. 2005; Arslanov 1994; Sidorovich et al. 2002; Kuznetsov et al. 2004). First studies of the Langmuir–Blodgett films based on cellulose esters with the alkyl substituents have been described in (Kawauchi et al. 1985; Shaub et al. 1995). The aliphatic CEs are used in the production of biodegradable plastics (Wang and Tao 1995; Edgar et al. 2001), membrane materials (Yang et al. 1998; Kuznetsov et al. 2004), and reinforcing agents for composites (Jandura et al. 2001).

Numerous attempts to produce chemically pure cellulose using ecologically safe technologies resulted, for example, in mastering the use of the cottonseed shell (Cheng et al. 2011), rice husk and hemp stems (Virtanen et al. 2012), cotton cloth waste (Ratanakamnuan et al. 2012), and agricultural waste (Kongruang 2008) as sources for production of CE.

The feasibility of attaching various side radicals to the backbone cellulose chain, which substantially change characteristics of polymer molecules (Tsvetkov et al. 1993), stimulates further study of these compounds. The molecular characteristics of CE essentially affect the surface properties of the samples under study. For example, it was shown (Kosaka et al. 2007) that elongation of the alkyl ester group leads to decrease in the surface energy of the Langmuir–Blodgett films and weakening of the Van der Waals interaction. The aliphatic cellulose esters belong to the vast class of rigid-chain polymers, whose study by the molecular hydrodynamic and optical methods have been carried out for a fairly long time and made it possible to obtain valuable data on the structural and conformational properties of the polysaccharide derivatives (Tsvetkov 1989).

It is important to emphasize that variation in the structure of the side substituents results in essential changes in the conformational characteristics of CE (Tsvetkov 1989). However, anisotropy of the optical polarizability of the monomeric unit of the chain, which is a sensitive indicator of its structure (Tsvetkov et al. 1999) is even more sensitive to the changes in the structure of the side substituents. Thus, the elongation of the side radicals in comb-like polymers leads to reduction of the positive anisotropy of the optical polarizability of the chain, reversal of its sign, and increase in its negative value, as is the case with polymethylmethacrylates (Tsvetkov et al. 1979).

In this work, we study the hydrodynamic, optical, and electrooptical properties of cellulose pelargonates (CP), tridecanoates (CTD), valerates (CV), and

acetovalerates (CAV) by the molecular hydrodynamic and optical methods.

Experimental

Materials

In our work, celluloses from evolutionarily different origins were used for the synthesis of cellulose esters. They are: long staple cotton, cotton linter, rice straw, wood, microcrystalline and algal cellulose (obtained from the White Sea algae *Cladophora rupestris*), animal cellulose (obtained from tunics of *Styelidae* ascidians (White Sea)), bacterial cellulose of *Gluconacetobacter xylinus* (synthesized in our laboratory using the strain GX CALU no. 1629 and standard CGX nutrient medium). Algal, animal and bacterial celluloses were purified by repeated boiling in 0.5–1.5 % NaOH solution and the following washing with water.

The synthesis of individual and mixed esters of these celluloses was performed using the mixed anhydride method in trifluoroacetic acid (TFA) medium; trifluoroacetic anhydride (TFAA) was used as a promoter, as described previously (Bourne et al. 1949; Hamalainen et al. 1957; Khripunov et al. 1970).

The esters were synthesized in the reaction of cellulose with the corresponding chemically pure acids in the presence of TFA and TFAA at the boiling temperature of the mixture for 90 min; the usual molar ratio cellulose: esterifying acid was 1:1, the TFA:TFAA ratio was 5:1. The product was precipitated in NaHCO₃ solution, washed with water at boiling temperature in order to remove the remaining TFA, and extracted with ethanol to remove unreacted esterifying acid.

The side substituents in the CP and CTD macromolecules are formed by the moieties of pelargonic acid [CH₃–(CH₂)₇–CO–] and tridecane acid [CH₃–(CH₂)₁₁–CO–], respectively, and in CV and CAV macromolecules by the isomers of valeric acid [C₆O₂H₇(OH)_{3–x–y}R₁xR₂y], where R₁: [CH₃–(CH₂)₃–CO–] is *n*-valerate, [(CH₃)₂CH–CH₂–CO–] is *iso*-valerate, [(CH₃)₃C–CO–] is pivalinate, and R₂: [CH₃–CO–] is the residue of acetic acid.

The values of the degree of substitution γ per 100 chain units of individual esters were established using elemental analysis (carbon, oxygen and hydrogen content) and by NMR in the case of mixed esters.

For the studied CP and CTD samples, the γ values are listed in Tables 1, 2, respectively. For the CV and CAV samples, the average degree of substitution by the valeric acid ($\gamma = 180$) was determined in (Bushin et al. 2009). The samples differ in origin (they are obtained from bacterial, wood pulp, cotton, linter, microcrystalline, animal, algae, and straw celluloses).

The molecular weights of the recurrent units of macromolecular chains M_0 were calculated according to their chemical structure and degree of substitution γ .

Chloroform (CF, refractive index $n = 1.4455$, permittivity $\varepsilon = 4.806$, density $\rho = 1.49 \text{ g} \times \text{cm}^{-3}$, dynamic viscosity $\eta_0 = 0.54$ centipoise), dioxane (DO, $n = 1.4262$, $\varepsilon = 2.209$, $\rho = 1.03 \text{ g} \times \text{cm}^{-3}$, $\eta_0 = 1.2$ centipoise), and tetrachloroethane (TCE,

$n = 1.4968$, $\varepsilon = 8.2$, $\rho = 1.59 \text{ g} \times \text{cm}^{-3}$, $\eta_0 = 1.69$ centipoise) were chosen as solvents.

Methods

The intrinsic viscosities $[\eta]$ were measured using the Ostwald capillary viscometer according to the standard technique (Tsvetkov 1989). In the capillary viscometers, the solvent outflow times lie within 50–80 s. To stabilize temperature, the viscometer was placed in a transparent bath of a thermostat, in which the temperature was varied within 21–51 °C during measurements. The error of the solution viscosity measurements did not exceed 5 %. The temperature

Table 1 Hydrodynamic characteristics of the CP samples in chloroform

Ser.no. ^a	γ	$[\eta]$, Dl \times g ⁻¹	$\alpha_n \times 10^3$, K ⁻¹	$D \times 10^7$, cm ² \times s ⁻¹	$-s_0$, Sv	M_0 , g \times mol ⁻¹	$M_{SD} \times 10^{-5}$, g \times mol ⁻¹	Z	$A_0 \times 10^{10}$, erg \times K ⁻¹
1	280	2.80	-5.1	1.1	15.3	556	8.9	1,600	2.7
2	200	2.00	-5.7	1.5	16.2	442	6.5	1,470	3.0
3	228	2.60	-1.3	1.4	14.4	481	6.2	1,290	3.0
4	255	2.12	-6.3	1.8	17.7	521	6.1	1,170	3.6
5	230	2.40	-2.9	1.4	13.2	487	5.7	1,170	2.8
6	228	2.90	-4.3	1.7	14.1	481	5.0	1,040	3.5
7	260	1.80	-5.0	2.3	10.8	519	2.8	540	3.3
8	240	1.34	-2.6	2.7	7.4	500	1.7	340	3.0
9	290	0.45	-1.9	3.9	7.2	550	1.1	200	2.6

^a The sources of cellulose are: for 1—linter, 2—algae, 3—animal, 4 and 5—cotton, 6—bacterial, 7—wood pulp, 8—straw, 9—microcrystalline

Table 2 Hydrodynamic characteristics of the CTD samples in chloroform

Ser.no. ^a	γ	$[\eta]$, Dl \times g ⁻¹	$\alpha_n \times 10^3$, K ⁻¹	$D \times 10^7$, cm ² \times s ⁻¹	$-s_0$, Sv	M_0 , g \times mol ⁻¹	$M_{SD} \times 10^{-4}$, g \times mol ⁻¹	Z	$A_0 \times 10^{10}$, erg \times K ⁻¹
1	240	2.90	-6.3	1.3	24.0	633	92	1,455	3.2
2	203	2.00	-5.4	1.4	17.0	561	60	1,066	2.7
3	237	1.75	-5.2	2.4	16.0	657.5	34	536	3.6
4	165	0.70	-4.7	3.6	10.0	486	14	288	3.0
5	225	0.45	-5.6	3.1	10.0	610	17	277	2.3
6	205	0.38	-8.9	3.9	8.5	564	11	194	2.4
7	165	0.65	-	4.6	8.1	486	8.8	181	3.2
8	200	0.39	-3.6	4.0	7.1	554	8.9	160	2.3
9	215	0.33	-3.0	5.0	8.0	584	8.0	138	2.6

^a The sources of cellulose are: for 1—linter, 2—cotton, 3—wood pulp, 4 and 7—bacterial, 5, 6 and 9—microcrystalline

Table 3 Hydrodynamic characteristics of CV and CAV in tetrachloroethane

Ser. no. ^a	Cellulose valerate	$M \times 10^{-4}$, $\text{g} \times \text{mol}^{-1}$	$[\eta]$, $\text{Dl} \times \text{g}^{-1}$ TCE	$[\eta]$, $\text{Dl} \times \text{g}^{-1}$ CF	$\Delta n/\Delta c \times 10^{10}$, $\text{g}^{-1} \times \text{cm} \times \text{s}^{2e}$
1	Aceto- <i>n</i> -valerate	26.9 ^b	1.06	1.93	−4.65
2	Aceto- <i>n</i> -valerate	12.5 ^c	0.89	2.55 ^d	−3.95
3	Aceto- <i>iso</i> -valerate	48.5 ^d	1.90	2.20 ^d	+0.17
4	<i>Iso</i> -valerate	24.7 ^b	1.15	1.79	+0.34
5	<i>n</i> -valerate	30.7 ^b	1.90	2.17	−5.0
6	Pivalinate	23.4 ^d	1.14	2.00	−
7	Pivalinate	22.8 ^b	1.56	1.66	−0.72
8	Pivalinate	4.05 ^d	0.46	0.43	−

^a The source for all samples N^o1–8 is linter

^b The molecular weights are calculated by the Mark-Kuhn-Houwink equation for chloroform $[\eta] = 2.5 \times 10^{-3} M^{0.9}$

^c The molecular weights are calculated by Eq. (4)

^d The values were determined in (Bushin et al. 2009)

^e Increment of the refractive index of the polymer-solvent system $dn/dc = 0.01 \text{ cm}^3 \times \text{g}^{-1}$

Table 4 Hydrodynamic, optical, and electrooptical characteristics of CP

Ser. no.	Solvent	$[\eta]$, $\text{Dl} \times \text{g}^{-1}$	$M_{\text{SD}} \times 10^{-5}$, $\text{g} \times \text{mol}^{-1}$	$\Delta n/\Delta c \times 10^{10}$, $\text{g}^{-1} \times \text{cm} \times \text{s}^{2a}$	$K \times 10^{10}$, $\text{g}^{-1} \times \text{cm}^5 \times (300 \times V)^{-2}$
1	CF	2.8	8.9	−10.1	−0.13
	DO	2.5	8.9	−6.3	−0.47
2	CF	2.0	6.6	−3.1	−0.41
	DO	3.0	6.6	−1.2	−
3	CF	2.6	6.2	−15.1	−
	DO	3.1	6.2	−7.3	−0.16
4	CF	2.1	6.1	−8.2	−0.44
	DO	3.3	6.1	−7.5	−0.77
5	CF	2.4	5.7	−5.9	−3.00
	DO	3.7	5.7	−5.8	−0.37
6	CF	2.9	5.0	−5.2	−0.72
	DO	3.3	5.0	−4.3	−0.36
7	CF	1.8	2.8	−9.5	−0.96
	DO	1.7	2.8	−7.7	−0.24
8	TCE	1.4	2.8	−7.0	−
	CF	1.3	1.7	−8.4	−3.56
9	DO	1.9	1.7	−4.0	−0.37
	CF	0.5	1.1	−8.9	~0
	DO	0.4	1.1	−7.2	−0.16

^aIncrement of the refractive index of the polymer-solvent system in CF $dn/dc = 0.04 \text{ cm}^3 \times \text{g}^{-1}$, in DO $dn/dc = 0.05 \text{ cm}^3 \times \text{g}^{-1}$ in TCE $dn/dc = 0.01 \text{ cm}^3 \times \text{g}^{-1}$

viscosity coefficients $\alpha_\eta = d\ln[\eta]/dT \times 10^3$ were determined for CP and CTD in CF. The obtained α_η values are listed in Tables 1, 2. The $[\eta]$ values for CP, CTD, CV, and CAV in various solvents are presented in Tables 1, 2, 3, 4, 5.

The diffusion coefficients D were measured in CF using a polarization diffusimeter (Tsvetkov 1989) by the solution-solvent interface spreading method. We used a glass cell 3 cm long along the light beam path at 24 °C. The solution concentration c did not exceed

Table 5 Hydrodynamic and optical characteristics of CTD in TCE

Ser. no.	$[\eta]$, $\text{Dl} \times \text{g}^{-1}$	$M_{\text{SD}} \times 10^{-4}$, $\text{g} \times \text{mol}^{-1}$	$\Delta n/\Delta t \times 10^{10}$, $\text{g}^{-1} \times \text{cm} \times \text{s}^{2\text{a}}$
1	0.26	8.0	−1.0
2	0.29	8.9	−8.0
3	0.39	8.8	–
4	0.35	11	−6.4
5	0.24	17	−8.6
6	0.32	14	−7.4
7	1.11	34	−12.4
8	0.89	60	−10.2
9	1.11	92	−13.1

^a Increment of the refractive index of the polymer-solvent system $dn/dc = 0.02 \text{ cm}^3 \times \text{g}^{-1}$

$0.1 \times 10^{-2} \text{ g} \times \text{cm}^{-3}$, which corresponds to the virtually limiting condition $c \rightarrow 0$. The photographs of the corresponding experimental interference fringes obtained using the polarization diffusimeter at different instants were processed by the method of maximum ordinates and areas under the concentration gradient curves (Tsvetkov et al. 1979). The diffusion coefficients $D = \sigma^2/2t$ were found from the slope of the straight lines of the dependence of the dispersion of the concentration boundary σ^2 on the diffusion time t . The error of the determination of the diffusion coefficients did not exceed 10 %. The obtained D values for CP and CTD are presented in Tables 1, 2, respectively.

The flotation coefficients ($-s$) for the CP and CTD samples in chloroform were determined on a MOM analytical ultracentrifuge (model 3180/B, Hungary) equipped with a polarization interferometric attachment (Tsvetkov 1989). We used a cell with polyamide insert allowing artificial boundary formation. The rotor speed was 40×10^3 rpm. The measurements were carried out at a temperature of 24 °C. The flotation coefficients s (s has a negative sign) were calculated using the equation $s = \omega^{-2} \times (d \ln(x)/dt)$, where ω is the angular velocity of the rotor and x is the coordinate of the maximum of the concentration gradient curve in the region of the flotation boundary, obtained from the slopes of the experimental linear dependences of $\ln(x)$ on the flotation time t . Thereby the dependences of the flotation coefficient s were determined. The concentration varied from 0.12 to $0.5 \times 10^{-2} \text{ g} \times \text{cm}^{-3}$. The linear dependences of $1/s$ on c were also determined according to the equation $1/s = (1/s_0)(1 + K_s c)$. The error of the determination of the flotation coefficients s_0 was within 10 %.

The flotation coefficients extrapolated to the zero concentrations s_0 for CP and CTD are presented in Tables 1, 2, respectively.

The molecular weights M of the samples were calculated by the Svedberg equation $M_{\text{SD}} = RT \cdot (|s_0|/D) \cdot (\bar{v}\rho_0 - 1)^{-1}$ using the measured diffusion coefficients D and flotation coefficient s_0 . The partial specific volumes of the polymers \bar{v} are $0.946 \text{ cm}^3 \times \text{g}^{-1}$ (CTD, CV, CAV) and $1.012 \text{ cm}^3 \times \text{g}^{-1}$ (CP). The obtained values of the molecular weights of CP, CTD, CV, and CAV are presented in Tables 1, 2, 3, respectively.

The refractive indices of the solutions and solvents were determined using a METTLER TOLEDO refractometer (model RM40, Switzerland) to the accuracy of $10^{-4} \pm 5 \times 10^{-5}$.

The dynamic flow birefringence (Maxwell effect) was studied in a dynamooptimeter with an inner rotor 3 cm in diameter and 3.21 cm in height. The gap between the stator and the rotor was 0.022 cm. To enhance the sensitivity, we used a photoelectric detection circuit with modulation of the light polarization ellipticity (Tsvetkov 1989; Tsvetkov and Andreeva 1981) and a semiconductor laser (HLDPM 12.655.5, wavelength $\lambda \approx 655 \text{ nm}$) as a light source. The elliptical rotary compensator provided the relative path difference $\Delta\lambda/\lambda = 0.04$. The dynamic flow birefringence was measured at a temperature of 24 °C maintained by forced water thermostating of the device. The error of the determination of the optical shear coefficient when using the above described technique did not exceed 10 % and was caused mainly by possible uncertainties in determination of the flow velocity gradient and in measurement of the device geometry, as well as by variations in the

Table 6 Optical characteristics of CP, CTD, CV, and CAV in various solvents

Solvent	$\Delta n/\Delta\tau_\infty \times 10^{10}, \text{g}^{-1} \times \text{cm} \times \text{s}^2$	$dn/dc, \text{cm}^3 \times \text{g}^{-1}$	$(\alpha_1 - \alpha_2) \times 10^{25}, \text{cm}^3$	S	$\Delta a \times 10^{25}, \text{cm}^3$
Cellulose tridecanoates					
TCE	-10.3	0.02	-130	42	-3.1
Cellulose pelargonates					
DO	-6.26	0.05	-80	40	-2.0
CF	-8.30	0.04	-100	35	-2.9
TCE	-7.00	0.01	-90	30	-3.0
Cellulose valerates and acetovalerates					
DO	+2.80	0.04	+36	46	+0.79
TCE	-4.50	0.01	-55	24	-2.3

The relative errors for the values listed in the table do not exceed 12 %

temperature at which the experiments were carried out.

The equilibrium electrical birefringence (Kerr effect) was studied in squared-pulsed (Tsvetkov et al. 1983) and sine-pulsed (Lezov and Tsvetkov 1990) electric fields. To enhance the sensitivity, we used the same photoelectric detection circuit as that described above for measuring the dynamic flow birefringence, but the elliptical rotary compensator provided the relative path difference $\Delta\lambda/\lambda = 0.01$ in this case. The measurements were made in a glass Kerr cell with titanium electrodes 3 cm in length along the light beam path and 0.03 cm interelectrode gap. The relative error of the K determination should be estimated from its sources, that are, first, the errors of the rotation angle of the compensator (commonly, $<2\%$), second, the error of the solution concentration ($<3\%$), and, third, the error of the voltage measurement (when using oscilloscope C8-13, the error is commonly $<5\%$). Hence, the estimated relative error of the K determination is within 10 %.

Results and discussions

Molecular-hydrodynamic and conformational characteristics of cellulose pelargonate and tridecanoate

The dependences of $M_0[\eta]$ ($\text{DI} \times \text{mol}^{-1}$), D , and $|s_0|/M_0$ on the degree of polymerization of samples Z ($Z = M/M_0$, where M_0 is the molecular weight of the recurrent unit of the molecular chain) in the interval $Z = 130\text{--}1,600$ for the solutions in CF are depicted in

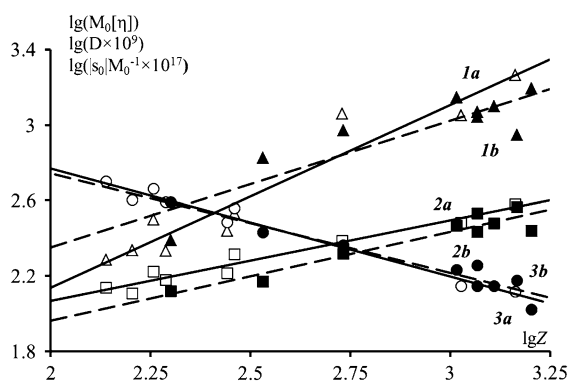


Fig. 1 Dependences of $\lg(M_0[\eta])$ (1), $\lg(|s_0|/M_0^{-1} \times 10^{17})$ (2) and $\lg(D \times 10^9)$ (3) on $\lg(Z)$ for the CTD (a) and CP (b) samples in chloroform

Fig. 1 on the logarithmic scale. The straight lines approximating these dependences are described by the Mark-Kuhn-Houwink equations at a temperature of 24 °C.

for CP:

$$\begin{aligned} M_0[\eta] &= 10.1Z^{0.67 \pm 0.04}, \\ D &= 6.20 \times 10^{-6} Z^{-0.52 \pm 0.02}, \\ |s_0|/M_0 &= 1.10 \times 10^{-16} Z^{0.47 \pm 0.02}, \end{aligned} \quad (1)$$

and for CTD:

$$\begin{aligned} M_0[\eta] &= 1.60Z^{0.97 \pm 0.04}, \\ D &= 8.25 \times 10^{-6} Z^{-0.57 \pm 0.02}, \\ |s_0|/M_0 &= 1.60 \times 10^{-16} Z^{0.43 \pm 0.02}. \end{aligned} \quad (2)$$

The obtained Eqs. (1) and (2) are typical for the cellulose esters (Tsvetkov 1989). The negative temperature coefficients of the intrinsic viscosities

(Tables 1, 2) is due to significant equilibrium rigidity and percolation of the molecules. This gives rise to increase in the exponents in the equations for $[\eta]$ and D as compared to the value of 0.5. The excluded-volume effects are small and virtually do not influence the values of the hydrodynamic characteristics or their dependence on Z .

For tetrachloroethane solvent, the Mark-Kuhn-Houwink equation for the viscosity has the following form:

$$\text{for CTD } M_0[\eta] = 3.4 \times Z^{0.73 \pm 0.05} \quad (3)$$

$$\text{for CV and CAV } M_0[\eta] = 6.2 \times Z^{0.62 \pm 0.04}. \quad (4)$$

The smaller exponent in the Mark-Kuhn-Houwink equation for the viscosity in tetrachloroethane as compared to that in chloroform indicates a more compact conformation of the CTD polymer macromolecules in this solvent. Similar situation is observed for the CV and CAV macromolecules (the Mark-Kuhn-Houwink equation for the chloroform solvent was obtained in (Bushin et al. 2009)).

Tables 1, 2, 3, 4 and 5 comprise the degree of substitution γ of the samples, intrinsic viscosities $[\eta]$, temperature viscosity coefficients α_η , diffusion coefficients D , flotation coefficients ($-s_0$), molecular weights of the recurrent chain units M_0 ; molecular weights of the samples M_{SD} , degree of polymerization Z ; the Tsvetkov–Klenin constant $A_0 \equiv \eta_0 D (M [\eta] / 100)^{1/3} / T$ (Tsvetkov and Klenin 1953), optical shear coefficient $\Delta n / \Delta \tau$, and the Kerr constant K .

To analyze the conformational properties of the cellulose ester molecules under study, we used the hydrodynamic theories of wormlike chains without excluded-volume effects (Norisuye et al. 1979; Yamakawa and Fujii 1973). According to these theories, the quantities $(f/M)^{-1} = DM/kT$ (specific molecular mobility, where f is the molecular friction coefficient) and $(M[\eta])^{1/3}$ (where $M[\eta]$ is the molecular volume) under ideal conditions are linear functions of $M^{1/2}$ at sufficiently large M corresponding to the molecular weights of the studied samples. The friction coefficient f of a molecule is proportional to its linear size: $f \sim (M[\eta])^{1/3}$; hence, $DM/kT \sim (M^2/[\eta])^{1/3} \sim M^{1/2}$.

The A_0 values are small and fluctuate around mean values of $(3.05 \pm 0.25) \times 10^{-10}$ and $(2.8 \pm 0.4) \times 10^{-10} \text{ erg} \times \text{K}^{-1}$ for CP and CTD, respectively. For CV and CAV the mean value of A_0 is $3.1 \times 10^{-10} \text{ erg} \times \text{K}^{-1}$ (Bushin et al. 2009).

The introduction of the proportionality factor A_{0m}/R (A_{0m} is the mean experimental value of the Tsvetkov–Klenin constant and R is the universal gas constant) made it possible to collate experimental data of viscometric and diffusion measurements and to use their collection as a unified system (Bushin et al. 1981).

Figure 2 shows the experimental values of $\eta_0 D Z / RT = [s] / M_0$ (1) (where $[s]$ is the intrinsic value of the sedimentation coefficient) and $(A_{0m}/R) \times (Z^2 / [\eta] M_0)^{1/3}$ (2) as a function of $Z^{1/2}$ for CTD in chloroform. The experimental data are fitted to the theoretical curve (Norisuye et al. 1979).

$$(N_A \lambda P_\infty)^{-1} \Psi(Z\lambda/A; d/A) \times (Z\lambda/A)^{1/2} = F(Z^{1/2}), \quad (5)$$

where function $\Psi(Z\lambda/A; d/A)$ is obtained from the ratio of the coefficient P in the translational friction theory and its limiting value $P_\infty = 5.11$ at $Z\lambda/A \rightarrow \infty$ (Norisuye et al. 1979), $Z\lambda/A$ is the number of the statistical chain segments, d/A is the relative diameter of the segment, A is the segment length, and d is its diameter. In the calculation, we used the length of the monomeric unit of β 1-4 glucans ($\lambda = 5.15 \times 10^{-8} \text{ cm}$).

Using Fig. 2, the equilibrium rigidity and hydrodynamic diameter of CP and CTD in chloroform were identified as $A = (18 \pm 2) \text{ nm}$, $d = (4 \pm 2) \text{ nm}$ and $A = (28 \pm 3) \text{ nm}$, $d = (2.0 \pm 0.5) \text{ nm}$ for CP and CTD, respectively. The obtained values of the hydrodynamic diameter d of the studied cellulose esters are sufficiently large, which is consistent with the small quantities of the hydrodynamic invariant A_0 (Tsvetkov et al. 1982) obtained above for these polymers.

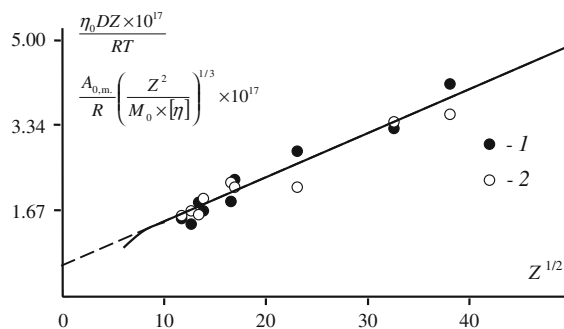


Fig. 2 Dependences of $\eta_0 D Z / RT = [s] / M_0$ (1) and $A_{0m} / R \times (Z^2 / [\eta] M_0)^{1/3}$ (2) on $Z^{1/2}$ for CTD in chloroform

Table 7 Conformational characteristics of the macromolecules in various solvents

Solvent	A, nm	σ	$\langle \cos \varphi \rangle$	$U_0 \times 10^{-3}$, $J \times \text{mol}^{-1}$	$\alpha_s \times 10^3$, K^{-1}	$\langle \cos^2 \varphi \rangle$	$dU_0/dT \times 10^{-3}$, $J \times \text{mol}^{-1} \times \text{K}$
Cellulose tridecanoates							
CF	28	4.8	0.92	31	-5.7	0.86	-0.054
TCE	22	4.3	0.89	25	-	-	-
Cellulose pelargonates							
DO	21	4.2	0.89	24	-	-	-
CF	18	3.9	0.87	21	-3.1	0.80	+0.017
TCE	15	3.5	0.85	18	-	-	-
Cellulose valerates and acetovalerates							
DO	24	4.4	0.90	27	-	-	-
CF	16	3.7	0.86	19	-7.7	0.78	-0.055
TCE	13	3.2	0.82	16	-	-	-

The relative errors for the values listed in the Table do not exceed 12 %

The values of the equilibrium rigidity are presented in Table 7.

It should be noted that no appreciable effect of the CTD origin on its hydrodynamic characteristics in diluted solutions is revealed in Fig. 2. Similar situation is also characteristic of the hydrodynamic properties of CP, CV and CAV, and the optical properties of all the macromolecules studied.

From the dependences of $(A_{0,m}/R) \times (Z^2/[\eta]M_0)^{1/3}$ on $Z^{1/2}$ similar to those shown in Fig. 2, we determined A for the studied macromolecules of CP in DO, CTD in TCE, CV and CAV in CF and TCE by the equation.

$$\begin{aligned} \frac{\eta_0 DZ}{RT} &= \frac{A_0}{R} \left(\frac{Z^2}{M_0[\eta]} \right)^{1/3} \\ &= (PN_A)^{-1} \left(\frac{Z}{\lambda A} \right)^{1/2} \\ &\quad + (3\pi N_A)^{-1} \left(\ln \frac{A}{d} - 1.0561 \right), \end{aligned} \quad (7)$$

where M_0 is the molecular weight of the monomeric unit, constant $P = 5.11$ (Yamakawa, Yoshizaki Yamakawa and Yoshizaki 1980). The Kuhn segment lengths calculated from the slopes of the straight lines are given in Table 7. The hydrodynamic invariant A_0 in TCE is assumed to be equal to 2.8×10^{-10} erg K^{-1} , as well as in CF.

The molecular-mass dependences of the translational diffusion or intrinsic viscosity for CP in TCE and CV in DO have not been studied in this work. So the equilibrium rigidity for these polymers in

mentioned solvents (which is necessary for the subsequent interpretation of the data on dynamic flow birefringence) was estimated by the A values in CF using the Flory equation $[\eta] = \Phi \times (LA)^{3/2} M^{-1}$, where $\Phi = 2.87 \times 10^{23}$ mol^{-1} (Yamakawa and Yoshizaki 1980). The characteristic viscosity ratio is given by the equation.

$$\frac{[\eta]_{CF}}{[\eta]_{solv}} = \left(\frac{A_{CF}}{A_{solv}} \right)^{3/2}, \quad (8)$$

where $[\eta]_{solv}$ and A_{solv} are the viscosity and rigidity, respectively, in the corresponding solvent (Table 6).

Table 6 gives the limit values (at $M \rightarrow \infty$) of the shear optical coefficient $(\Delta n/\Delta \tau)_\infty$ which were obtained by averaging the experimental values of $\Delta n/\Delta \tau_\infty$ for the most of high-molecular weight samples. Also Table 6 comprises the optical anisotropy of the molecular segments α_1 – α_2 , the number of the monomeric units in the Kuhn segment S, and the optical anisotropy of the monomeric units Δa .

It should be noted that the equilibrium rigidity of the polymer chains of the studied macromolecules decreases when a nonpolar solvent is replaced by a polar one. This is brought about by the fact that the intramolecular hydrogen bonds play the essential role in the mechanism of the formation of the equilibrium rigidity of the cellulose ester macromolecules. The interactions between the side groups can be weakened under the influence of the polar molecules of a solvent capable of forming intermolecular links. This specific feature is exhibited not only in the hydrodynamic

properties of cellulose derivatives, but is no less distinctly manifested in the dynamic flow birefringence effect (Tsvetkov 1989; Tsvetkov et al. 1993; 1990).

The values of the degree of hindrance were determined from the equation $\sigma = (A/A_f)^{1/2}$, where A is the length of the Kuhn segment and $A_f = 1.2$ nm is the length of the Kuhn segment when the rotation is unhindered in the polysaccharide chain (Tsvetkov 1989). The σ values for the cellulose esters studied are presented in Table 7. These values agree well with the data obtained earlier for other cellulose derivatives in various solvents (from 3.2 to 4.8; for cellulose, 2.6) (Tsvetkov 1989) and also decrease as the solvent polarity increases. The obtained σ values indicate significant stabilization of the intramolecular bond structure of the skeleton chain whose flexibility corresponds to small deformation vibrations about the rotation bonds of its oxygen bridges.

According to the theory of the deformation flexibility of the structures with coplanar arrangement of the rotational bonds, the mean value $\langle \cos \varphi \rangle$

$$\langle \cos \varphi \rangle = \frac{\int_0^\pi \exp[-U_0(1 - \cos \varphi)/2RT] \cos \varphi \, d\varphi}{\int_0^\pi \exp[-U_0(1 - \cos \varphi)/2RT] \, d\varphi} \quad (9)$$

is defined by the activation energy U_0 of the *trans*–*cis* transition in the configuration of the effective rotational bonds of the three recurrent units of the polyglucoside chain. The mean $\langle \cos \varphi \rangle$ value of the azimuth φ of the intramolecular rotations about the oxygen bridge bonds of the polyglucoside chain was calculated by the equation (Taylor 1947; Kuhn 1947; Benoit 1948).

$$\sigma^2 = (1 + \langle \cos \varphi \rangle) / (1 - \langle \cos \varphi \rangle). \quad (10)$$

The degree of hindrance σ , the mean $\langle \cos \varphi \rangle$ value of the azimuth φ of the intramolecular rotations about the oxygen bridge bonds of the polyglucoside chain, the energy of hindrance of the internal rotations U_0 , the temperature coefficient of the unperturbed size of the macromolecule α_s , and the activation potential dU_0/dT of the studied cellulose esters in various solvents are presented in Table 7.

The U_0 value for CV and CAV exceeds the values of the hindrance energy potentials of the internal rotations about the bonds of the ordinary flexible chain polymers (Flory 1969; Tsvetkov et al. 1979). For CP and CTD U_0 is close to the energy of strong

intramolecular interactions (electrostatic, hydrogen bonds) that occur in other cellulose esters (Tsvetkov 1989; Tsvetkov et al. 1993; Jbankov and Kozlov 1983). The obtained U_0 values indicate a substantial (dominating) role of the steric interactions of the long aliphatic side substituents in the molecule rigidity stabilization of the studied cellulose ester samples.

Intramolecular interactions in macromolecules of TDC and PC define not only the high value of the energy U_0 , but also the temperature changes in the sizes of the unperturbed chains $\langle h^2 \rangle$ and in the energy U_0 itself. To determine the temperature coefficient of the unperturbed chain size $\alpha_s = d \ln \langle h^2 \rangle / dT$ and the energy of hindrance of the intramolecular rotations dU_0/dT of the CP and CTD macromolecules in chloroform, we proposed the method based on the study of the molecular mass dependences of the temperature coefficients of intrinsic viscosity α_n , presented in Fig. 3.

The values of $(M^2/[\eta])^{1/3}$ (line 1) and $(M^2/[\eta])^{1/3} d \ln [\eta] / dT$ (line 2) as functions of $M^{1/2}$ are presented in Fig. 3 for CP (a) and CTD (b) in chloroform. The approximating lines (1) and (2) are drawn through the aggregate of points according to the equations (Bushin et al. 1981).

$$\begin{aligned} (M^2/[\eta])^{1/3} &= \Phi^{-1/3} (M_0/A\lambda)^{1/2} M^{1/2} + 0.73 \\ &\times \Phi^{-1/3} (M_0/\lambda) \cdot [\ln(A/d) - 0.75] \end{aligned} \quad (11)$$

$$\begin{aligned} (M^2/[\eta])^{1/3} d(\ln[\eta]/dT) &= \Phi^{-1/3} (3/2) \times \alpha_s \\ &\times (M_0/A\lambda)^{1/2} M^{1/2} - 2.2 \\ &\times \Phi^{-1/3} (M_0/A\lambda) \\ &\times d \ln(A/d) / dT, \end{aligned} \quad (12)$$

where the second equation is the derivative of the first one with respect to temperature. The temperature coefficients of the unperturbed macromolecule size were determined from the ratio of the angular coefficients $\Phi^{-1/3} (3/2) \times \alpha_s \times (M_0/A\lambda)^{1/2}$ and $\Phi^{-1/3} (M_0/A)^{1/2}$ of lines (2) and (1) in Fig. 3, which is equal to $(3/2)\alpha_s$. For CP and CTD $\alpha_s = d \ln \langle h^2 \rangle / dT = -3.1 \times 10^{-3}$ and $-5.7 \times 10^{-3} \text{ K}^{-1}$, respectively. For CV and CAV $\alpha_s = -7.7 \times 10^{-3} \text{ K}^{-1}$ was determined in (Bushin et al. 2009). According to the rigid chain nature of the macromolecules, the equilibrium rigidity and unperturbed chain size decrease as temperature T increases.

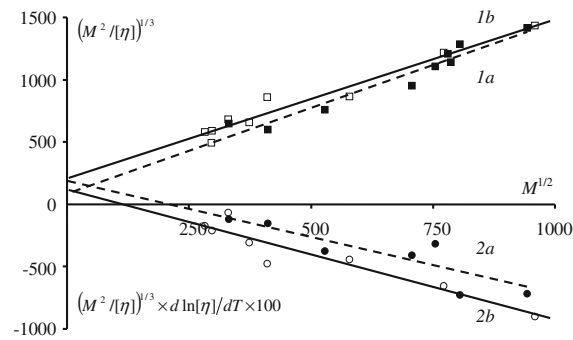


Fig. 3 The values of $(M^2/[\eta])^{1/3}$ (1) and $(M^2/[\eta])^{1/3} d\ln[\eta]/dT$ (2) as functions of $M^{1/2}$ for CP (a) and CTD (b) in chloroform

Using the equation (Tsvetkov et al. 1993)

$$\alpha_s = (RT)^{-1} \times (-U_0/T + dU_0/dT) \cdot [(\langle \cos^2 \phi \rangle - \langle \cos^2 \phi \rangle^2) / (1 - \langle \cos^2 \phi \rangle^2)] \quad (13)$$

and calculating $\langle \cos^2 \phi \rangle$ according to the equation

$$\langle \cos^2 \phi \rangle = \frac{\int_0^\pi \exp[-U_0(1 - \cos \phi)/2RT] \cos^2 \phi d\phi}{\int_0^\pi \exp[-U_0(1 - \cos \phi)/2RT] d\phi}, \quad (14)$$

with the values of $U_0 = 21.0$, 30.9 and $19.0 \text{ kJ} \times \text{mol}^{-1}$ for CP, CTD, and CV and CAV, respectively, we determined $\langle \cos^2 \phi \rangle$ and dU_0/dT for CP, CTD and CV in chloroform. The activation potential U_0 of CTD undergoes decrease comparable with its drop in the cases of cellulose acetocinnamate (CAC) ($dU_0/dT = -0.057 \text{ kJ} \times \text{mol}^{-1} \times \text{K}$ (Tsvetkov et al. 1993)) and cellulose valerate ($dU_0/dT = -0.055 \text{ kJ} \times \text{mol}^{-1} \times \text{K}$ (Bushin et al. 2009)), which either do not contain substituents at all (CAC) or contain short aliphatic substituents (valeric acid residue as a side substituent at a moderate value of $\gamma = 180$). On the contrary, the positive values of $dU_0/dT = +0.034$ and $+0.017 \text{ kJ} \times \text{mol}^{-1} \times \text{K}$ are characteristic of cellulose acetomyristate (CAM) and CP, respectively, which are polymers with a high density of the aliphatic substituents along the chain.

An increase in the interaction energy U_0 with temperature can be attributed to unfolding of the aliphatic chains and increasing the volume of the aliphatic phase that frames the skeleton cellulose chain.

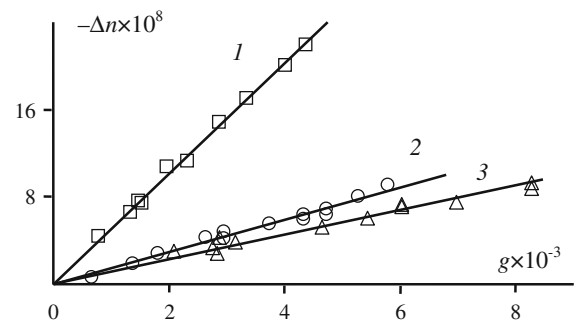


Fig. 4 The birefringence Δn as a function of the flow velocity gradient g (s^{-1}) for the CTD sample No. 1 in TCE. $c \times 10^2$ ($\text{g} \times \text{cm}^{-3}$): 1–0.65, 2–0.32, 3–0.25

Optical properties of cellulose pelargonate, tridecanoate, valerate, and acetovalerate

To study the optical characteristics of cellulose esters, we chose TCE as a solvent due to the fact that the refractive index increment does not exceed $0.02 \text{ cm}^3 \times \text{g}^{-1}$ for CTD in TCE. Hence, the role of the optical micro- and macroform effects is negligibly small in this case. We determined the proper values of the optical shear coefficient, optical anisotropy of the Kuhn segment, and optical anisotropy of the monomeric unit of the polymers studied in TCE. Figure 4 shows the birefringence Δn as a function of the flow velocity gradient g for the CTD sample No. 1 in TCE for three concentrations of the polymer solution. It can be seen from Fig. 4 that these dependences are linear. The dependences of the birefringence Δn on the shear stress $\Delta\tau$ ($\Delta\tau = g(\eta - \eta_0)$, where η and η_0 are the viscosities of solution and solvent, respectively) for

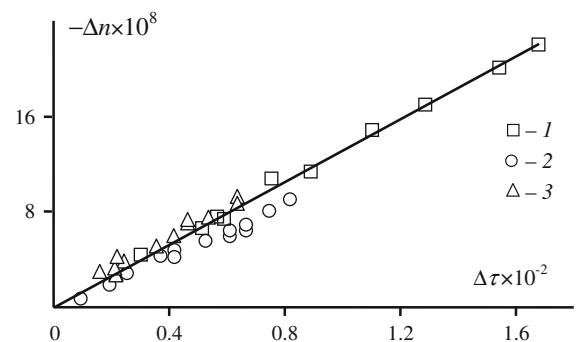


Fig. 5 The birefringence Δn as a function of the shear stress $\Delta\tau$ ($\text{g} \times \text{cm}^{-1} \times \text{s}^{-2}$) for the CTD sample No. 1 in TCE. $c \times 10^2$ ($\text{g} \times \text{cm}^{-3}$): 1–0.65, 2–0.32, 3–0.25

the same sample are depicted in Fig. 5. The points pertaining to various concentrations are extrapolated well by a single straight line, which indicates the concentration independence of the optical shear coefficients of the studied polymers. Similar results were observed for the other CP, CTD, CV, and CAV samples as well. The optical shear coefficients $\Delta n/\Delta\tau$ for the studied samples, which are presented in Tables 3, 4, 5, were determined from the obtained experimental dependences.

The optical shear coefficient is negative for all CP and CTD samples studied. This is caused by the negative contributions of the aliphatic side substituents to the optical anisotropy of the studied polymer macromolecules and negligibly small influence of the optical effects of micro- and macroform. The latter fact arises from the insignificant increment of the refractive index of the polymer–solvent system (for the solutions in CF and TCE).

Taking into account the substantial molecular mass of the majority of the studied samples, their macromolecules can be considered as Gaussian coils. Then, the optical anisotropy of the molecular segment (α_1 – α_2) of the studied cellulose esters can be determined using the well-known Kuhn equation (Tsvetkov et al. 1979):

$$\Delta n/\Delta\tau = \frac{4\pi}{45kT} \frac{(n_s^2 + 2)^2}{n_s} (\alpha_1 - \alpha_2), \quad (15)$$

where n_s is the refractive index of the solvent, T is the absolute temperature, and k is the Boltzmann constant. The values of α_1 – α_2 averaged over all the samples studied are presented in Table 6.

The value of the optical anisotropy of the monomeric unit Δa is calculated by the equation

$$\Delta a = (\alpha_1 - \alpha_2)/S, \quad (16)$$

where $S = A/\lambda$ is the number of the monomeric units in the Kuhn segment.

The values of the optical shear coefficient $\Delta n/\Delta\tau$ and the optical anisotropy of the monomeric unit Δa depend on the refractive index n_s of the solvent, which is primarily associated with the manifestation of the microform effect in the observed birefringence. Thus, some decrease of the optical anisotropy of the monomeric unit of CP in dioxane can be noted.

The optical shear coefficient $\Delta n/\Delta\tau = +2.8 \times 10^{-10} \text{ g}^{-1} \times \text{cm} \times \text{c}^2$ was also determined for the CV sample no. 5 (*n*-valerate) in dioxane. The obtained values of the optical anisotropy of the molecular

segments and the optical anisotropy of the monomeric unit of CV in dioxane are presented in Table 6. The positive sign of the optical anisotropy is due to the contribution of the microform effect.

As noted above, the increment of the refractive index of the polymer-solvent system is extremely small for TCE; hence, the obtained Δa value can be considered to be the intrinsic optical anisotropy of the monomeric unit Δa_i . The data that we obtained correlate well with the results of the earlier study of other cellulose esters with the aliphatic side substituents (Tsvetkov 1989; Tsvetkov et al. 1995).

It is of interest to compare the calculated Δa values with those obtained earlier for the aliphatic cellulose esters series (Tsvetkov et al. 1995). The negative Δa values for CP, CTD, CV, and CAV appear to be larger in magnitude than these for cellulose acetates and butyrates, but smaller than these for cellulose myristinates.

The intrinsic optical anisotropy Δa_i as a function of the number of carbon atoms v in the side substituent attached to the ester group is presented in Fig. 6. Dots are the experimental data for cellulose acetates, butyrates, valerates and acetovalerates, pelargonates, and tridecanoates, respectively, and the curve is the theoretical dependence calculated by the equation.

$$\Delta a_i = -\frac{1}{16} n \Delta b \left[1 - e^{-6v/n} \right] \quad (17)$$

This equation defines the optical anisotropy of a wormlike chain in terms of the axes of the first element (Tsvetkov 1989; Tsvetkov et al. 1995) with due account of the tilt angle of the first element of the side

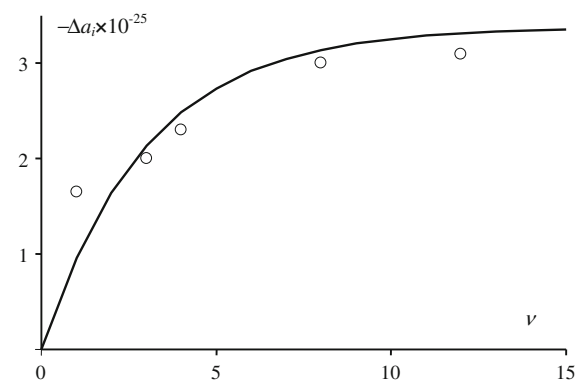


Fig. 6 The intrinsic optical anisotropy of the monomeric unit Δa_i of the cellulose esters as a function of the number of carbon atoms v in a side radical (attached to the ester group)

chain with respect to the backbone chain being equal to 60° . The experimental data are best fit to the theoretical dependence at the following choice of parameters (notwithstanding a noticeable spread primarily arising from the extremely small values of Δa for the cellulose esters with aliphatic side substituents): $\Delta b = 3.0 \times 10^{-25} \text{ cm}^3$ (anisotropy per single valence bond in the aliphatic chain) and $n = 18$ (the number of valence bonds in the Kuhn segment for the aliphatic chain). These values agree well with Δb and n for the polyethylene chain (Tsvetkov 1989).

The obtained result is an indication that the interactions between the side substituents in CP, CTD, CV, and CAV macromolecules in the solvents do not lead to decrease in the extent of convolution of the side chains, as is quite often the case in the comb-like polyacrylates and polymethylmethacrylates (Tsvetkov 1989). The obtained results corroborate the inference made in the previous study (Tsvetkov et al. 1995) that the optical anisotropy of the cellulose esters with the aliphatic side radicals is governed only by the side substituents of a macromolecule, whereas the optical anisotropy of the cellulose chain with the attached ester groups is close to zero.

Electrooptical properties of cellulose pelargonate and valerate

The CP solutions were studied by the method of the equilibrium electrooptic effect. The results obtained by the method of the equilibrium Kerr effect are illustrated in Fig. 7, which shows the dependences of

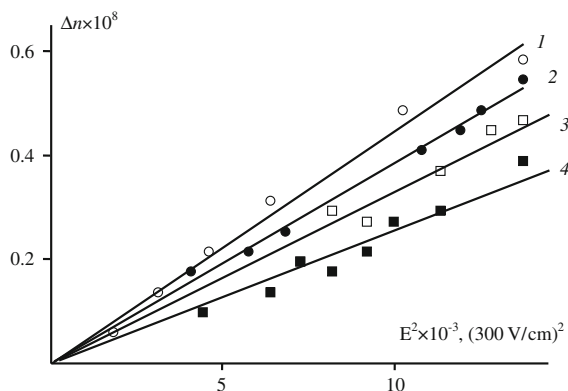


Fig. 7 Dependence of the electrooptic effect Δn on the squared rectangular-pulsed field strength E^2 for CP samples in dioxane. CP samples: 2—no. 5, 3—no. 9, and 4—no. 7; $c \times 10^2$ ($\text{g} \times \text{cm}^{-3}$): 2—0.24, 3—0.93, 4—0.82. 1—pure dioxane

the electrooptic effect Δn on the squared rectangular-pulsed field strength E^2 for some CP samples in dioxane at various concentrations c of the polymer solutions. The linear dependence indicates the applicability of the Kerr law. Similar dependences were observed for all CP studied in all solvents used. The specific Kerr constants K_c were determined for the studied polymers from the obtained experimental data using the equation.

$$K_c = \frac{(\Delta n_d - \Delta n_s)}{cE^2}, \quad (18)$$

where Δn_d and Δn_s are the electrooptic birefringences of the solution and solvent, respectively.

The Kerr constants for all studied samples did not exhibit monotonic concentration dependence (in the cases when we succeeded in measurements at several concentrations). Therefore, the characteristic Kerr constant $K = \lim_{c \rightarrow 0} K_c$ was assumed to be the K_c value at the lowest c . The K values for the studied CP are listed in Table 4.

The coincidence of the signs of the electrooptic effect and the birefringence of the studied CP is an evidence of the identical mechanisms of reorientation of their macromolecules in the external electric and hydrodynamic fields in dioxane and chloroform that occurs according to the large-scale motion mechanism irrespective of the solvent properties, which is characteristic of the rigid-chain polymers (Tsvetkov 1989; Tsvetkov and Tsvekov 1993).

Taking into account significant molecular weights of the most of the studied samples, we believe that the Kerr constant for these samples can be described by the equation for a worm-like kinetically rigid coil K_∞ (Tsvetkov and Tsvekov 1993), which is valid in the Gaussian limit (the reduced chain length $x \rightarrow \infty$).

$$K_\infty = \left(\frac{2B\Delta a}{M_0} \right) \mu_0^2 S^2 \cos^2 \vartheta, \quad (19)$$

where Δa is the optical anisotropy of the polymer monomeric unit and B is the Lorentz internal field factor

$$B = \left(\frac{\pi N_A}{1215(kT)^2 n} \right) (n^2 + 2)^2 (\varepsilon + 2)^2 \quad (20)$$

From Eqs. (19) and (20), we determined the value of the longitudinal component of the dipole of the monomeric unit $\mu_{0||} = \mu_0 \times \cos \theta$, where θ is the angle

of the dipole direction of the monomeric unit with the chain direction. Equation (19) is almost identical to that obtained in a recent work for semiflexible wormlike chains in the limit $x \rightarrow \infty$ (see Eqs. 47 and 54 in Garsia de la Torre et al. (2010)).

The estimates of $\mu_{0||}$ are reasonable only when nonpolar solvents are used and the Lorentz and Onsager internal field factors coincide (Tsvetkov 1990). The value of the longitudinal component of the dipole of the monomeric unit in nonpolar dioxane obtained thereby amounts to $\mu_{0||} = 0.4 \pm 0.1$ D for the studied CP samples.

For one of the CV samples (no. 5) in dioxane we obtained the optical shear coefficient $\Delta n/\Delta\tau = +2.8 \times 10^{-10} \text{ g}^{-1} \times \text{cm} \times \text{s}^2$ and the specific Kerr constant $K = +0.087 \times 10^{-10} \text{ g}^{-1} \times \text{cm}^5 \times (300 \times \text{V})^{-2}$. From Eq. (19), we also estimated the value of the longitudinal component of the dipole of the monomeric unit in nonpolar dioxane for CV: $\mu_{0||} = 0.2 \pm 0.1$ D.

These values are close to those obtained earlier (Tsvetkov et al. 1995) for various cellulose esters with the aliphatic side substituents. This is due to the fact that the dipole structure of the cellulose esters with the aliphatic side substituents is governed by their backbone chain (with the attached ester groups) and is independent of the length of the aliphatic substituents which do not contain the polar groups.

Conclusions

The equilibrium rigidities of polymers in dioxane, chloroform and trichloroethane are determined by the molecular hydrodynamics methods. It is demonstrated that the equilibrium rigidities of macromolecules decrease as the solvent polarity and temperature increase. The rigidity of the studied polymers, as well as of the other cellulose esters, is governed by the hindered rotation about valence bonds due to interaction of the side groups.

The intrinsic anisotropy of the monomeric units of cellulose tridecanoates, pelargonates, valerates, and acetoverates has been experimentally determined. The aliphatic side substituents make negative contribution to the optical anisotropy of the studied polymer macromolecules. The longitudinal component of the dipole moment of the monomeric units of CP, CV and CAV coincides with that obtained for other cellulose esters with the aliphatic side substituents. The dipole

structure of cellulose esters with the aliphatic side substituents is governed by their backbone chain with the attached ester groups.

The conformational, optical, and electrooptical properties of the CP, CTD, CV and CAV macromolecules are well correlated with these characteristics of cellulose esters with the aliphatic side substituents studied earlier.

References

- Arslanov VV (1994) Polymer monolayers and Langmuir-Blodgett films. The influence of the chemical structure of the polymer and of external conditions on the formation and properties of organized planar assemblies. *Russ Chem Rev* 63:1–39. doi:10.1070/RC1994v063n01ABEH000069
- Benoit H. (1948) Calcul de l'écart quadratique moyen entre les extrémités de diverses chaînes moléculaires de type usuel. *J Pol Sci* 3:376–388. doi:10.1002/pol.1948.120030312
- Borgan RT and Brewer RJ (1985) Cellulose esters, organic. In: Kroschwitz JI (ed) *Encyclopedia Polymer Science and Technology*, 2nd edn. Wiley, New York. 3:158–181
- Bourne EJ, Stacey M, Tatlow JC, Tedder JM (1949) Studies on trifluoroacetic acid. Part I. Trifluoroacetic anhydride as a promoter of ester formation between hydroxy-compounds and carboxylic acids. *J Chem Soc* 2976–2979. doi:10.1039/JR9490002976
- Bushin SV, Tsvetkov VN, Lysenko YeB, Yemel'yanov VN (1981) The sedimentation-diffusion and viscometric analysis of the conformation properties and molecular rigidity of ladder-like polyphenyl siloxane in solution. *Polym Sci USSR* 23:2705–2715. doi:10.1016/0032-3950(81)90043-5
- Bushin SV, Khripunov AK, Astapenko EP, Bezrukova MA (2009) Hydrodynamic and conformational properties of cellulose valerate molecules in dilute solution. *Polym Sci A* 51:761–769. doi:10.1134/S0965545X09070025
- Cheng HN, Dowd MK, Shogren RL, Biswas A (2011) Conversion of cotton byproducts to mixed cellulose esters. *Carbohydr Polym* 86:1130–1136. doi:10.1016/j.carbpol.2011.06.002
- Edgar KJ, Buchanam CM, Debenham JS, Rundquist PA, Seiler BD, Shelton MC, Tindall D (2001) Advances in cellulose ester performance and application. *Prog Polym Sci* 26:1605–1688. doi:10.1016/S0079-6700(01)00027-2
- Flory PJ (1969) *Statistical Mechanics of Chain Molecules*. John Wiley & Sons, New York
- Garsia de la Torre J, Dias Banos FG, Peres Sanchez HE (2010) Kerr constant of multi-subunit particles and semiflexible, wormlike chains. *J Phys: Condens Matter* 22:494104. doi:10.1088/0953-8984/22/49/494104
- Hamalainen C, Wade RH, Buras EM (1957) Fibrous cellulose esters by Trifluoroacetic anhydride method. *Text Res J* 27:168. doi:10.1177/004051755702700211
- Jandura P, Kokta BV, Riedl B (2001) Cellulose fibers/polyethylene hybrid composites: effect of long chain organic acid cellulose esters and organic peroxide on rheology and

- tensile properties. *J Reinf Plast Compos* 20(8):697–717. doi:[10.1177/07316840172679048](https://doi.org/10.1177/07316840172679048)
- Jbankov RG, Kozlov PV (1983) Physics of cellulose and its derivatives. Nauka I tehnika, Minsk
- Kawaguchi T, Nakahara H, Fukuda K (1985) Monomolecular and multimolecular films of cellulose esters with various alkyl chains. *Thin Solid Films* 133:29–38. doi:[10.1016/0040-6090\(85\)90422-5](https://doi.org/10.1016/0040-6090(85)90422-5)
- Khripunov AK, Kozmina OP, Shtennikova IN, Ohrimenco GI (1970) Cellulose esters and aliphatic-aromatic acids. *Rus J Appl Chem* 43:2581–2583 (in rus.)
- Khripunov AK, Baklagina YuG, Denisov VM, Volkov AY, Lavrent'ev VK, Stepina ND, Yanusova LG, Feigin LA (2000) Model of packing of cellulose acetomyristinate in Langmuir-Blodgett films. *Crystallogr Rep* 45:318–322. doi:[10.1134/1.171189](https://doi.org/10.1134/1.171189)
- Klemm D, Philipp B, Heinze T, Heinze U, Wagenknecht W (1998) *Comprehensive Cellulose Chemistry*. Wiley-VCH Verlag, Germany
- Kongruang S (2008) Bacterial cellulose production by Acetobacter xylinum strains from agricultural waste products. *Appl Biochem Biotechnol* 148:245–256. doi:[10.1007/s12010-007-8119-6](https://doi.org/10.1007/s12010-007-8119-6)
- Kosaka PM, Kawano Y, Petri DFS (2007) Dewetting and surface properties of ultrathin films of cellulose esters. *J Colloid Interface Sci* 316:671–677. doi:[10.1016/j.jcis.2007.07.058](https://doi.org/10.1016/j.jcis.2007.07.058)
- Kuhn H (1947) Restricted bond rotation and shape of unbranched saturated hydrocarbon chain molecules. *J Chem Phys* 15:843–844. doi:[10.1063/1.1746348](https://doi.org/10.1063/1.1746348)
- Kuznetsov YuP, Khripunov AK, Kruchinina EV, Kuznetsov VM, Turkova LD, Pen'kova AV (2004) Transport properties of cellulose ester membranes for separating gas and liquid mixtures. *Rus J Appl Chem* 77:1877–1882. doi:[10.1007/s11167-005-0180-8](https://doi.org/10.1007/s11167-005-0180-8)
- Lezov AV, Tsvetkov NV (1990) Methods of investigation measurement of Kerr effect by means of sinusoidal impulses as a tool for studying the dynamics of macromolecules in conductive solutions. *Polym Sci USSR* 32:162–165. doi:[10.1016/0032-3950\(90\)90064-D](https://doi.org/10.1016/0032-3950(90)90064-D)
- Norisuye T, Motowoka M, Fujita H (1979) Wormlike chains near the rod limit: translational friction coefficient. *Macromol* 12:320–323. doi:[10.1021/ma60068a032](https://doi.org/10.1021/ma60068a032)
- Ratanakamnuan U, Atong D, Aht-Ong D (2012) Cellulose esters from waste cotton fabric via conventional and microwave heating. *Carbohydr Polym* 87:84–94. doi:[10.1016/j.carbpol.2011.07.016](https://doi.org/10.1016/j.carbpol.2011.07.016)
- Shaub M, Fakirov C, Schmidt A, Lieser G, Wenz G, Werner G, Albouy PA, Wu H, Foster MD, Majrzkak C, Satija S (1995) Ultrathin layers and supramolecular architecture of isopentylcellulose. *Macromol* 28:1221–1228. doi:[10.1021/ma00108a059](https://doi.org/10.1021/ma00108a059)
- Sidorovich AV, Baklagina YuG, Khripunov AK, Bursian AE, Denisov VM, Lavrent'ev VK, Praslova OE, Kuznetsov YuP, Kruchinina EV, Shtykova EV, Sukhanova TE (2002) Structure and transport properties of films of mixed cellulose esters. *Rus J Appl Chem* 75:1700–1704. doi:[10.1023/A:1022204507634](https://doi.org/10.1023/A:1022204507634)
- Steinmeier H (2004) Chemistry of cellulose acetylation. *Macromol Symp* 208:49–60. doi:[10.1002/masy.200450405](https://doi.org/10.1002/masy.200450405)
- Stepina ND, Klechkovskaya VV, Yanusova LG, Feigin LA, Tolstikhina AL, Sklizkova VP, Khripunov AK, Baklagina YuG, Kudryavtsev VV (2005) Formation of Langmuir-Blodgett films in solutions of comblike polymers. *Crystallogr Rep* 50:614–624. doi:[10.1134/1.1996736](https://doi.org/10.1134/1.1996736)
- Taylor WJ (1947) Average square length and radius of unbranched long-chain molecules with restricted internal rotation. *J Chem Phys* 15:412–414. doi:[10.1063/1.1746540](https://doi.org/10.1063/1.1746540)
- Tredgold RH (1987) The physics of Langmuir-Blodgett films. *Rep Prog Phys* 50:1609–1656. doi:[10.1088/0034-4885/50/12/002](https://doi.org/10.1088/0034-4885/50/12/002)
- Tsvetkov VN (1989) *Rigid-Chain Polymers*. Consult Bur Plenum NY, London
- Tsvetkov NV (1990) Kerr Effect in polar solvents. *Vestnik LGU* 4:22–30 (in rus)
- Tsvetkov VN, Andreeva LN (1981) Flow and electric birefringence in rigid-chain polymer solutions. *Adv Polym Sci* 39:95–207. doi:[10.1007/3-540-10218-3_3](https://doi.org/10.1007/3-540-10218-3_3)
- Tsvetkov VN, Klenin SI (1953) Diffusion of polystyrene fractions in dichloroethane. *Doclady Akad Nauk SSSR* 88(1):49–52 (in rus)
- Tsvetkov VN, Tsvetkov NV (1993) Electrical birefringence in solutions of rigid-chain polymers. *Russ Chem Rev* 62:851–876. doi:[10.1070/RC1993v062n09ABEH000050](https://doi.org/10.1070/RC1993v062n09ABEH000050)
- Tsvetkov VN, Eskin VE, Frenkel SYa (1979) Structure of macromolecules in solutions. *Natl Lend Libr Sci Technol*, Boston Spa
- Tsvetkov VN, Lavrenko PN, Bushin SV (1982) A hydrodynamic invariant of polymeric molecules. *Russ Chem Rev* 51(10):975–993. doi:[10.1070/RC1982v051n10ABEH002935](https://doi.org/10.1070/RC1982v051n10ABEH002935)
- Tsvetkov VN, Kolomiets IP, Lezov AV, Stepchenkov AS (1983) Use of modulation of elliptic light polarization for the study of electric birefringence of polymer solutions in pulse fields. *Polym Sci USSR* 25:1541–1546. doi:[10.1016/0032-3950\(83\)90095-3](https://doi.org/10.1016/0032-3950(83)90095-3)
- Tsvetkov VN, Lezov AV, Tsvetkov NV, Andreeva LN (1990) Kerr effect in solutions of cellulose carbanilate in polar solvents. *Eur Polym J* 26:1103–1107. doi:[10.1016/0014-3057\(90\)90010-2](https://doi.org/10.1016/0014-3057(90)90010-2)
- Tsvetkov VN, Bushin CV, Bezrukova MA, Astapenko EP, Didenko SA, Khripunov AK, Denisov VM (1993) Hydrodynamic, dynamooptical, and conformational characteristics of molecules of cellulose acetocinnamate. *Vysokomolekulyarnye Soedineniya. A* 35(10):1632–1640 (in rus.)
- Tsvetkov VN, Khripunov AK, Astapenko EP, Didenko SA (1995) Optical and electrooptical properties of cellulose esters with aliphatic side groups. *Polym Sci A* 37:791–798
- Tsvetkov VN, Andreeva LN, Tsvetkov NV (1999) Anisotropy of segments and monomer units of polymer molecules. In: Brandrup J, Immergut EH, Grulke E (eds) *Polymer handbook*, 4th edn. Wiley J & Sons, New York, pp 745–763
- Virtanen T, Virtanen T, Svedström K, Andersson S, Knaapila M, Kotelnikova N, Maunu SL, Serimaa R (2012) A physico-chemical characterisation of new raw materials for microcrystalline cellulose manufacturing. *Cellul* 19:219–235. doi:[10.1007/s10570-011-9636-6](https://doi.org/10.1007/s10570-011-9636-6)
- Wang P, Tao BY (1995) Synthesis of cellulose-fatty acid esters for use as biodegradable plastics. *J Environ Polym Degrad* 3:115–119. doi:[10.1007/BF02067487](https://doi.org/10.1007/BF02067487)

- Yamakawa H, Fujii M (1973) Translational friction coefficient of wormlike chains. *Macromol* 6:407–415. doi:[10.1021/ma60033a018](https://doi.org/10.1021/ma60033a018)
- Yamakawa H, Yoshizaki T (1980) Transport coefficients of helical wormlike chains. 3. Intrinsic viscosity. *Macromology* 13(3):633–643. doi:[10.1021/ma60075a02](https://doi.org/10.1021/ma60075a02)
- Yang JS, Kim HJ, Jo WH, Kang YS (1998) Analysis of pervaporation of methanol-MTBE mixtures through cellulose acetate and cellulose triacetate membranes. *Polym* 39: 1381–1385. doi:[10.1016/S0032-3861\(97\)00416-3](https://doi.org/10.1016/S0032-3861(97)00416-3)